11-fs dark pulses generated via coherent absorption in plasmonic metamaterial

VENKATRAM NALLA,[1,*] JOÃO VALENTE,[2] HANDONG SUN,[1] AND NIKOLAY I. ZHELUDEV[1,2]

[1]*Centre for Disruptive Photonic Technologies, School of Physical and Mathematical Sciences, The Photonic Institute, Nanyang Technological University, Singapore*
[2]*Optoelectronics Research Centre and Centre for Photonic Metamaterials, University of Southampton, Highfield, Southampton, UK*
*vnalla@ntu.edu.sg

Abstract: We demonstrate generation of the shortest reported 11fs dark pulses using the coherent absorption process on a plasmonic absorber with a gating pulse. The dark pulses appear as a power dip on the envelope of a long carrier pulse and are characterized using the cross-correlation technique. The principal difference and advantage of our approach in comparison with previously developed laser sources of dark pulses is that, in principle, it allows transferring arbitrary pattern of bright pulses into a pattern of dark pulses in another optical signal channel.

References and links

1. A. Hasegawa and F. Tappert, "Transmission of stationary nonlinear optical pulses in dispersive dielectric fibers. I. Anomalous dispersion," Appl. Phys. Lett. **23**(3), 142–144 (1973).
2. D. Krökel, N. J. Halas, G. Giuliani, and D. Grischkowsky, "Dark-Pulse Propagation in Optical Fibers," Phys. Rev. Lett. **60**(1), 29–32 (1988).
3. A. M. Weiner, J. P. Heritage, R. J. Hawkins, R. N. Thurston, E. M. Kirschner, D. E. Leaird, and W. J. Tomlinson, "Experimental Observation of the Fundamental Dark Soliton in Optical Fibers," Phys. Rev. Lett. **61**(21), 2445–2448 (1988).
4. R. W. Schoenlein, S. Chattopadhyay, H. H. W. Chong, T. E. Glover, P. A. Heimann, C. V. Shank, A. A. Zholents, and M. S. Zolotorev, "Generation of Femtosecond Pulses of Synchrotron Radiation," Science **287**(5461), 2237–2240 (2000).
5. Y. S. Kivshar and B. Luther-Davies, "Dark optical solitons: physics and applications," Phys. Rep. **298**(2-3), 81–197 (1998).
6. D. J. Frantzeskakis, "Dark solitons in atomic Bose–Einstein condensates: from theory to experiments," J. Phys. A **43**(21), 213001 (2010).
7. X. Xue, Y. Xuan, Y. Liu, P.-H. Wang, S. Chen, J. Wang, D. E. Leaird, M. Qi, and A. M. Weiner, "Mode-locked dark pulse Kerr combs in normal-dispersion microresonators," Nat. Photonics **9**(9), 594–600 (2015).
8. D. Meshulach and Y. Silberberg, "Coherent quantum control of two-photon transitions by a femtosecond laser pulse," Nature **396**(6708), 239–242 (1998).
9. J. Zimmermann, S. T. Cundiff, G. von Plessen, J. Feldmann, M. Arzberger, G. Böhm, M.-C. Amann, and G. Abstreiter, "Dark pulse formation in a quantum-dot laser," Appl. Phys. Lett. **79**(1), 18–20 (2001).
10. M. Feng, K. L. Silverman, R. P. Mirin, and S. T. Cundiff, "Dark pulse quantum dot diode laser," Opt. Express **18**(13), 13385–13395 (2010).
11. H. H. Liu and K. K. Chow, "Dark pulse generation in fiber lasers incorporating carbon nanotubes," Opt. Express **22**(24), 29708–29713 (2014).
12. H. Zhang, D. Y. Tang, L. M. Zhao, and X. Wu, "Dark pulse emission of a fiber laser," Phys. Rev. A **80**(4), 045803 (2009).
13. A. M. Weiner, R. J. Hawkins, R. N. Thurston, W. J. Tomlinson, J. P. Heritage, D. E. Leaird, and E. M. Kirschner, "Temporal and spectral self-shifts of dark optical solitons," Opt. Lett. **14**(16), 868–870 (1989).
14. X. Li, S. Zhang, Y. Meng, and Y. Hao, "Harmonic mode locking counterparts of dark pulse and dark-bright pulse pairs," Opt. Express **21**(7), 8409–8416 (2013).
15. J. Liu, X. Li, S. Zhang, H. Zhang, P. Yan, M. Han, Z. Pang, and Z. Yang, "Polarization domain wall pulses in a microfiber-based topological insulator fiber laser," Sci. Rep. **6**(1), 29128 (2016).
16. W. Liu, L. Pang, H. Han, W. Tian, H. Chen, M. Lei, P. Yan, and Z. Wei, "Generation of dark solitons in erbium-doped fiber lasers based Sb2Te3 saturable absorbers," Opt. Express **23**(20), 26023–26031 (2015).

17. Y. D. Chong, L. Ge, H. Cao, and A. D. Stone, "Coherent Perfect Absorbers: Time-Reversed Lasers," Phys. Rev. Lett. **105**(5), 053901 (2010).
18. N. Liu, L. Langguth, T. Weiss, J. Kastel, M. Fleischhauer, T. Pfau, and H. Giessen, "Plasmonic analogue of electromagnetically induced transparency at the Drude damping limit," Nat. Mater. **8**(9), 758–762 (2009).
19. M. Papaioannou, E. Plum, J. Valente, E. T. F. Rogers, and N. I. Zheludev, "Two-dimensional control of light with light on metasurfaces," Light Sci. Appl. **5**(4), e16070 (2016).
20. C. Sönnichsen, T. Franzl, T. Wilk, G. von Plessen, J. Feldmann, O. Wilson, and P. Mulvaney, "Drastic Reduction of Plasmon Damping in Gold Nanorods," Phys. Rev. Lett. **88**(7), 077402 (2002).
21. J. Zhang, K. F. MacDonald, and N. I. Zheludev, "Controlling light-with-light without nonlinearity," Light Sci. Appl. **1**(7), e18 (2012).
22. L. F. Mollenauer and K. Smith, "Demonstration of soliton transmission over more than 4000 km in fiber with loss periodically compensated by Raman gain," Opt. Lett. **13**(8), 675–677 (1988).
23. W. Zhao and E. Bourkoff, "Propagation properties of dark solitons," Opt. Lett. **14**(13), 703–705 (1989).

1. Introduction

Dark pulses are sharp dips in power of electromagnetic radiation that are often accompanied by a phase jump across the intensity minimum. Since their first observation [1], dark pulses have attracted considerable attention, especially in the fields of solitons [2, 3], x-ray spectroscopy [4], nonlinear optics [5], Bose – Einstein condensation [6], optical communications [5], generation of Kerr combs [7] and coherent quantum control of optical transitions in atoms [8]. The generation of dark pulses of few hundreds of femtoseconds to nanoseconds duration has been demonstrated by various methods [3, 9–13]. These methods includes, spectral filtering by spatially patterned amplitude and phase masks [3], complex manipulation of regimes of ytterbium-doped fiber ring laser [14] and various other lasers with saturable absorbers based on carbon nanotubes [11], topological insulators [15], Antimony telluride films [16] and InGaAs:Be, Er doped multi-quantum wells [10]. The principal difference and advantage of our approach in comparison with previously developed laser sources of dark pulses is that, in principle it allows transferring arbitrary pattern of "bright" pulses into a pattern of "dark" pulses in another channel. Moreover, our relatively simple and robust method allows formation of dark pulse as short as only a few wave periods. Here we report generation of 11fs dark pulses using the effect of "perfect absorption" [17, 18]. When two coherent counter-propagating electromagnetic waves of the same intensity form a standing wave, a thin absorber placed in the antinode of the wave could completely dissipate energy of both waves if its traveling wave absorption is 50%. If one of the waves is a short "gate" pulse, the "perfect absorption" regime will lead to the depletion of energy from the other "carrier" wave during their temporal overlap on the absorber, creating a dark pulse.

2. Generation of femtosecond dark pulses

We use the "coherent perfect absorption" regime to generate a dark pulse on the profile of relatively long 70fs carrier pulse by dissipating its energy into plasmonic absorber during a short period of interference with an 11fs gate pulse, as illustrated schematically in Fig. 1. Pulses with 6fs duration and repetition rate of 75MHz are generated by a mode-locked Ti:sapphire laser (Femtolasers "Rainbow") and then conditioned to nearly transform-limited 11fs pulses by a pulse shaper (Biophotonics- MIIPS) by taking feedback at the sample position. The 11fs gate pulses with a central wavelength of 800nm and a spectral full-width half-maximum of around 85nm generated by the pulse shaper are split by a 50:50 pellicle beam splitter. In the carrier channel pulses are stretched from 11fs to 70fs using 10nm band pass filter (BPF). In the gate channel the pulses pass through a tunable attenuator comprising of a half wave plate (HWP) and a linear polarizer (LP). This attenuator is used to balance intensities of waves interacting at the absorbing film (similar intensities are used in both the channels, average power was measured by photo diode). To restore duration of the gate pulses after broadening in the attenuator, they are passed through a pair of dispersion compensation mirrors (DCM). Both beams are focused (diameter ~40μm) on the absorber from the opposite sides by two parabolic mirrors (FM – ROC ~15cm) forming a standing wave at the absorber's

location. Low pulse fluence, below 0.5 nJ/cm^2, was maintained during the experiment to minimize opto-thermal damage and nonlinear effects in the absorber.

As an absorber we used a free-standing plasmonic metamaterial film, a two-dimensional array of asymmetric split ring slits in a free-standing gold nano-membrane [Fig. 1(b)]. Starting from a 50nm thick silicon nitride membrane supported on a silicon frame, we thermally evaporated a 60nm thick gold film on a 50nm thick silicon nitride membrane supported on a silicon and then removed the silicon nitride layer by reactive ion etching, keeping the gold layer intact. Metamaterial pattern was then fabricated on the gold nano-membrane by focused ion beam milling. The overall size of the metamaterial array was 50µm × 50µm. The period of array in both directions (320nm) was shorter than any wavelength of light used in the experiment and therefore at normal incidence light does not diffract on the absorber. The resulting metamaterial 60nm in thickness showed a plasmonic resonance around 800nm with peak absorption of ~47% [Fig. 1(c)]. As the regime of perfect absorption requires the absorbing film to be placed exactly at the anti-node of the standing wave with sub-micron accuracy, piezo actuator was used to adjust absorber's position.
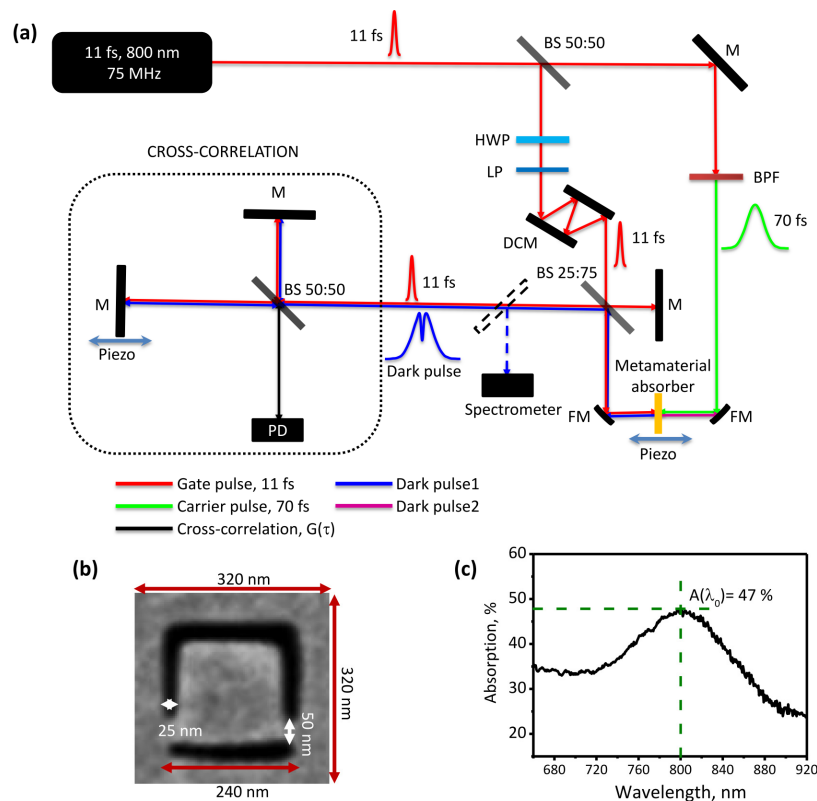

Fig. 1. Femtosecond "Dark pulse" generation via coherent perfect absorption in plasmonic metamaterial. (a) To generate a dip in the profile of "carrier" pulse, a metamaterial absorber is placed in the standing wave formed by the "carrier" and "gate" pulses. M-mirror, FM-focusing mirror, BS-beam splitter, HWP- half wave plate, LP- linear polarizer, DCM-dispersion compensated mirrors, BPF-band pass filter, PD- photo diode. (b) Single unit cell of metamaterial absorber. (c) Absorption spectra of the free-standing metamaterial absorber, $A(\lambda_0) = 47\%$ is absorption at 800 nm.

Spectral and temporal profiles of the "bright" pulses were characterized by spectrometer and by measuring their field cross-correlation (auto-correlation for 11fs) functions [Fig. 2 and Fig. 4]. This cross-correlator (auto-correlator) is calibrated with the standard FROG's data taken by pulse shaper. To characterise the dark pulses generated by perfect absorption, we

also measured a field cross-correlation function, $G(\tau) = \int_{-\infty}^{\infty} E_{dark\ pulse1}(t) E_{gate}(t-\tau)dt$ between the dark pulse and the gate pulse [Fig. 4(c)]. The correlator consisted of a beam splitter and two mirrors in the Michelson interferometer arrangement, where one of the mirrors was translated by a piezo drive and output of the correlator was monitored by integrating silicon detector [Fig. 1(a)].
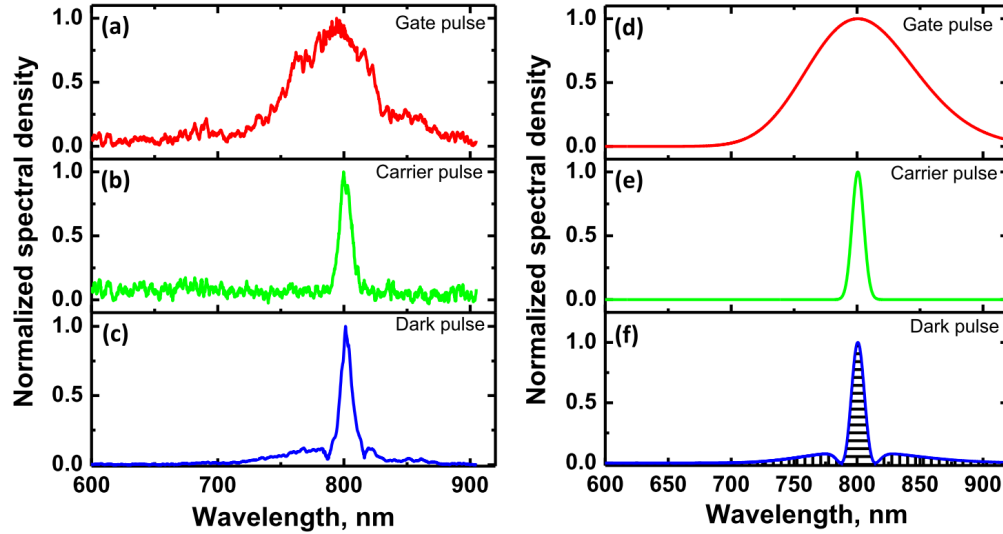

Fig. 2. Spectral profiles of gate, carrier and dark pulse, (a-c) experimental spectra, (d-f) simulated spectra. Red: 11fs gate pulse, green: 70fs carrier pulse and blue: dark pulse when sample is at anti-node (perfect coherent absorption).

To model the process of dark pulse generation we assume experimental values of absorption A(λ) as presented at Fig. 1(c), A(λ_0) = 0.47 at the peak. Here spectral components of the dark pulse can be calculated from the scattering matrix of the 4-port device handling two input waves (carrier and gate) and two output waves one of which corresponds to the dark pulse investigated in our experiment (dark pulse1) and another is from the opposite direction of the absorber (dark pulse2) [19]:

$$\begin{pmatrix} E_{dark\ pulse1}(\lambda) \\ E_{dark\ pulse2}(\lambda) \end{pmatrix} = \begin{pmatrix} s(\lambda) & (s(\lambda)+1) \\ s(\lambda)+1 & s(\lambda) \end{pmatrix} \begin{pmatrix} E_{gate}(\lambda) \\ E_{carrier}(\lambda) \end{pmatrix} \qquad (1)$$

where s = -A(λ), (s = −0.5 corresponds to the case of coherent perfect absorption for identical pulses). Assuming transform-limited Gaussian carrier and gate pulses, corresponding calculated spectral density profiles and modelled dark pulse alongside with experimental carrier and gate pulses are shown in Fig. 2. It is interesting to note that ~64% of 11fs dark pulse energy (shaded section of the spectrum, horizontal lines) is confined within the range of frequencies forming a much longer 70fs carrier pulse, while the remaining 36% of energy is spread over frequency range corresponding to the short 11fs gate pulse (shaded section of the spectrum, vertical lines).

As shown in Fig. 3(f), we also simulated the field cross-correlation function between the dark and gate pulse, as measured in the experiment [Fig. 4(c)]. The temporal profile of the simulated dark pulse corresponding to the cross-correlation function at Fig. 3(f) is presented at Fig. 3(c).
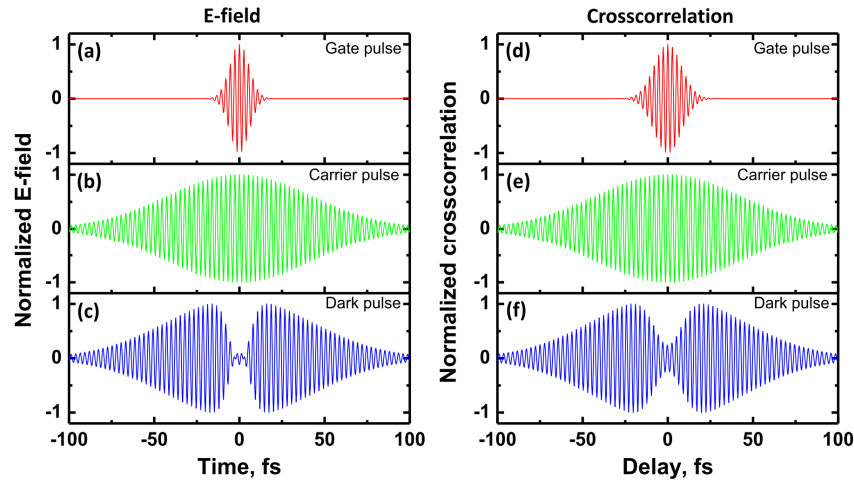
Fig. 3. Simulated dark pulse in the envelope of carrier pulse. (a-c) Electric fields of 11fs gate pulse, 70fs carrier pulse and dark pulse respectively; (d) Autocorrelation function of the 11fs gate pulse; (e-f) First order electric field cross-correlation function of the 11fs gate pulse with 70fs carrier pulse and dark pulse respectively.
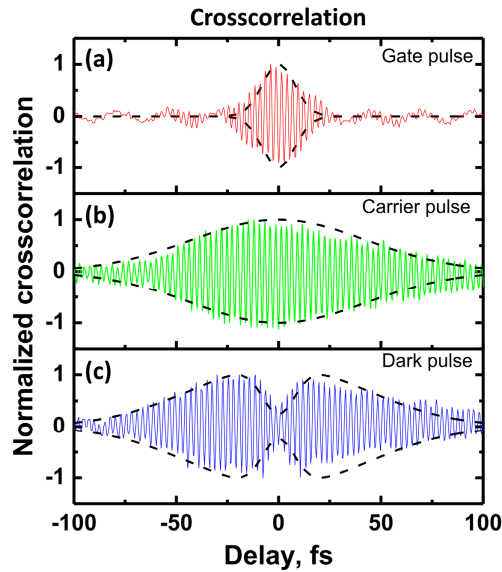

Fig. 4. Experimental data on the generation of dark pulse in the envelope of carrier pulse. (a) First order electric field auto-correlation function of the 11fs gate pulse; (b) cross-correlation function 70fs carrier pulse with gate pulse; (c) cross-correlation function of the dark pulse with gate pulse. Experimental data presented here is after subtracting the constant background. Dashed black lines are envelopes of simulated cross-correlation functions taken form Fig. 3.

Experimental cross correlation function presented at Fig. 4(c) corresponds to a dark pulse of 11fs duration. Our attempts to generate shorter dark pulses with gate pulses as short as 6fs have not resulted in shortening of dark pulses. 11fs pulses are arguably the shortest dark pulse duration possible with metamaterial plasmonic absorber made of gold metamaterial film as spectrum of absorption is limited by the width of the plasmonic response linked to the plasmon relaxation time in gold [20] [see Fig. 1(c)]: interaction of spectral components of shorter carrier and gate pulses outside of the absorption line will not lead to efficient coherent absorption. We have confirmed this independently by measuring the standing wave absorption of gate pulse as a function of pulse duration. This was performed in a simplified

version of interferometer when all elements of the interferometer apart from beam-splitter, focusing optic and metamaterial absorber were removed from the set up making arrangements for the perfect absorption experiment [21]. Results are presented in Fig. 5. They indicate that standing wave absorption indeed drops for pulses shorter than 11fs. We shall note here that slow decline of coherent absorption upon increase of pulse duration from 11fs to 185fs is explainable by onset of nonlinear effect of absorption saturation at high fluencies.
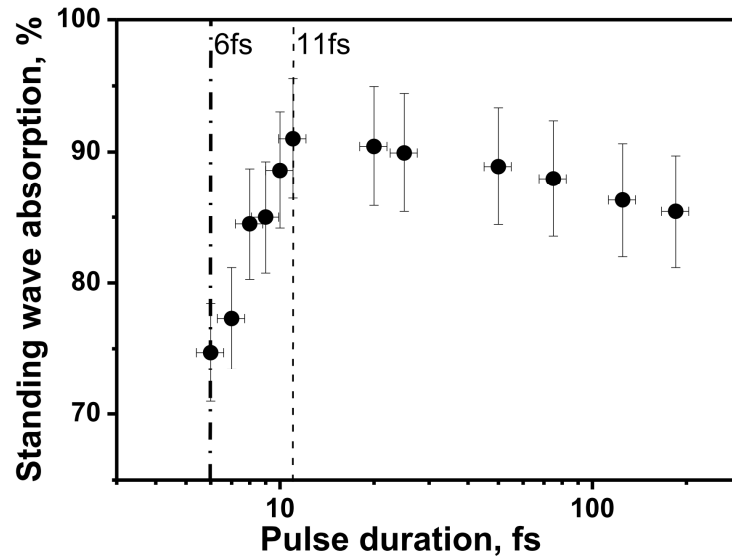

Fig. 5. Interaction with short pulses with thin absorber in the standing wave regime. Standing wave absorption as measured on plasmonic metamaterial at different pulse excitations.

3. Conclusions

In summary, we demonstrate generation of the shortest so far, 11fs dark pulses using the process of perfect coherent absorption in a thin plasmonic metamaterial. We also show that spectral width of the plasmonic absorption resonance that is linked to the plasmon relaxation time in gold does not allow generation of pulses shorter than 11fs using this type of absorbers. We argue that such pulse could enable the generation of short dark solitons which can propagate large distances in dispersive media without broadening [22] with high stability, low loss and low noise compared with bright solitons [16, 23]. Dark pulses also can be used in spectroscopy enabling direct measurement of ultra-short excitation dynamics [4].

Funding

Acknowledgments